Numerical simulation of fatigue crack growth with stress-strain relationship under cyclic loading

SHIMOOKA, Tsukasa
Department of Naval Architecture and Ocean Engineering, Graduate School of Engineering, Kyushu University : Master course student

MURAKAMI, Koji
Technical Division, School of Engineering, Kyushu University : Senior Technician

MATSUDA, Kazuki
Department of Marine Systems Engineering, Faculty of Engineering, Kyushu University : Associate Professor

GOTOH, Koji
Department of Marine Systems Engineering, Faculty of Engineering, Kyushu University : Professor

https://hdl.handle.net/2324/7157018

出版情報：Proceedings of The 36th Asian-Pacific Technical Exchange and Advisory Meeting on Marine Structures (TEAM 2023), pp.122-128, 2023-10-12
バージョン：

TEAM 2023, *October. 10 - 13, 2023, Busan, South Korea*

Numerical simulation of fatigue crack growth with stress-strain relationship under cyclic loading.

Tsukasa SHIMOOKA*[1], Koji MURAKAMI*[2], Kazuki MATSUDA*[3], Koji GOTOH*[4]

1) *Master course student, Department of Naval Architecture and Ocean Engineering, Graduate School of Engineering, Kyushu University; 744, Motooka, Nishi-ku, Fukuoka, 819-0395, Japan*
e-mail: shimoka.tsukasa.938@s.kyushu-u.ac.jp
2) *Senior Technician, Technical Division, School of Engineering, Kyushu University; 744, Motooka, Nishi-ku, Fukuoka, 819-0395, Japan*
e-mail: murakami.kouji.940@m.kyushu-u.ac.jp
3) *Associate Professor*, Department *of Marine Systems Engineering, Faculty of Engineering, Kyushu University; 744, Motooka, Nishi-ku, Fukuoka, 819-0395, Japan*
e-mail: matsuda@nams.kyushu-u.ac.jp
4) *Professor*, *Department of Marine Systems Engineering, Faculty of Engineering, Kyushu University; 744, Motooka, Nishi-ku, Fukuoka, 819-0395, Japan*
e-mail: gotoh@nams.kyushu-u.ac.jp

Abstract

In numerical simulations of fatigue crack propagation, the true stress-true strain relationship under cyclic loading should be considered, but in simulations modelling crack opening behaviour, the stress-strain relationship of the material is regarded as rigid plastic or isotropically hardened elastic-plastic material from the point of view of model simplification.

In this study, the true stress-true strain relationship under cyclic loading, estimated from the true stress-true strain relationship under monotonic tensile loading, is implemented in fatigue crack propagation simulations of work-hardened materials proposed by some of authors.

Fatigue crack growth curves under the following three loadings, (1) constant cyclic loading under different stress ratios, (2) two-stage block loading cycles, (3) constant cyclic loading with a spike load, were estimated and compared with the measured results obtained in previous studies.

The results show that the accuracy of the fatigue crack growth estimation is better than the conventional stress-strain relationship assuming elastic-perfectly plastic materials.

Keyword: Stress-strain diagrams under cyclic loading, Numerical simulation of fatigue crack propagation,

1. INTRODUCTION

Toyosada et al. [1] considered that the driving source of fatigue crack propagation is irreversibly consumed by both tensile and compressive plastic work in the alternative plastic zone near the crack tip, and proposed a Re-tensile Plastic zone's Generated load (RPG load) based fatigue crack propagation law that indirectly expresses this, showing the usefulness of this law under various variable loading conditions. In this propagation law, the stress range from the RPG load to the maximum load is considered as the effective stress range. Numerical simulations implementing this propagation law and a mathematical model of the crack opening and closing behaviour have also been developed, where the material is treated as elastic-plastic in this simulation. Yamashita et al [2] extended the numerical simulation of Ref. [1] and developed a numerical simulation that can consider the work hardening effect of the material. However, at this stage, the stress-strain relationship obtained from monotonic tensile tests was used as input.

In this crack growth analysis, it is desirable to input the stress-strain relationship under cyclic loading. Although there have been various reports on the stress-strain relationship under cyclic loading, the true stress-strain relationship, which should be input to the crack propagation analysis, has rarely been reported, partly because it is difficult to measure the true stress-strain relationship under cyclic loading, especially when the strain value becomes large. In recent years, however, advances in measuring instruments have made it possible to measure the history of changes in the minimum cross-sectional diameter and specimen curvature of (hourglass-shaped) round bar specimens under cyclic loading in a non-contact manner, making it relatively easy to measure the true stress-true strain history during cyclic loading. The authors [3] measured the true stress - true strain relationship under cyclic loading and showed that it is possible to estimate the stress-strain relationship under cyclic loading for hull structural steels only from the results of monotonic tensile tests.

In this paper, we propose a method to approximate the true stress-true strain diagram from the results of monotonic tensile test only. Then, the true stress-strain diagram under cyclic loading estimated by the authors was then implemented in a numerical fatigue crack growth simulation by Yamashita et al. [2]. Numerical simulations were then performed for fatigue crack growth tests under several loading histories and compared with the measured results [1]. The necessity of considering the material stress-strain relationship in the estimation of fatigue crack growth history is discussed.

2. OVERVIEW OF THE METHOD FOR ESTIMATING CYCLIC TRUE STRESS-STRAIN RELATIONSHIP

This chapter provides an overview of the authors' proposed method for estimating the stress-strain relationship under cyclic loading. The method is intended for hull structural steels and steels of similar material strength.

The mechanisms of yielding include intergranular dislocation yielding and intragranular dislocation yielding, and for normal steels the macroscopic yielding is said to be dominated by the mechanism with the higher critical stress. When ferritic steel is tempered and rolled, the yield point is lowered in the same way as in the cyclic tests, and this is thought to be due to a shift in mechanism from intergranular dislocation yielding to intragranular dislocation yielding.

On the other hand, cyclic yield stress (: σ_{y2}) can be expressed as in Eq. (1) using friction stresses (:σ_0) and dislocation strengthening (:$\Delta\sigma$).

$$\sigma_{y2} = \sigma_0 + \Delta\sigma \tag{1}$$

In polycrystalline metals, it is widely known that the Hall-Petch relationship, in which the yield stress is proportional to the inverse of the square root of the grain size *d* [mm], holds true, and for ferritic steels containing more than 50 ppm carbon, the value of the Hall-Petch coefficient is 6.0 x10^{-4} [MPa・$mm^{1/2}$] and is almost constant [4], the following equation holds for the static yield stress σ_{y1}.

$$\sigma_{y1} = \sigma_0 + (6.0 \times 10^{-4})/\sqrt{d} \text{ [MPa]} \tag{2}$$

The amount of dislocation strengthening based on in-grain dislocation yielding was devised by Akama et al. based on the Bailey-Hirsch relationship, using true strain ε_t and grain size *d* [mm], as estimated in Eq. (3) below [5], [6].

$$\Delta\sigma = 0.0307 \times \sqrt[4]{\varepsilon_t/d} \text{ [MPa]} \tag{3}$$

From Eqs. (1) to (3), the cyclic yield stress (:σ_{y2}) can be expressed using the static yield stress (:σ_{y1}) and grain size (:d) as in Eq. (4).

$$\sigma_{y2} = \sigma_{y1} - (6.0 \times 10^{-4})/\sqrt{d} + 0.0307 \times \sqrt[4]{\varepsilon_t/d} \text{ [MPa]} \tag{4}$$

Equation (4) allows the cyclic yield stress to be estimated simply by carrying out static monotonic tensile tests and grain size measurements.

To verify the validity of Eq. (4), grain size measurements were carried out on the same steel material that was subjected to cyclic testing in the previous chapter. The grain size measurements were based on the cutting method of JIS G 0551 [7]. The measurement results are shown in Table 3.

Table3 Grain size and Eq. (4) substitution results.

	grain size [mm]	Eq. (4) substitution results [MPa]
Average grain size	9.60 x 10^{-3}	310
Maximum grain size	1.62 x 10^{-2}	341
Mininmum grain size	4.84 x 10^{-3}	253

Substituting the grain size measurement results in Table 3 into Eq. (4) confirms the validity of this method of estimation, as the experimental values of cyclic yield stress fall within the range of the maximum and minimum grain size assignments.

The proposed equation is expressed in the following form with the plastic strain ε_{pl} as a parameter.

$$\sigma = F * \varepsilon_{pl}{}^{n} + \sigma_{y2} \tag{5}$$

1. Determine the cyclic yield stress σ_{y2} from Eq. (4).
2. Only the data range of total strain $\varepsilon_{total} \geq 0.05$ of the stress-strain relationship during monotonic tensile tests is used to determine the coefficient *F*, *n* by making a least-squares power approximation in the graph of the '$\sigma - \sigma_{y2}$' to 'ε_{pl}' relationship ('(true stress) minus (yield stress)' to 'plastic strain' relationship).

The cyclic stress-strain diagram produced based on the above procedure for the same material as the steel for which cyclic tests is shown in Fig. 1. Experimental values are also shown for comparison. In this case, the mean value of the grain size measurement and the yield strain of the static test are substituted, the cyclic yield stress is 315 MPa and *F* and *n* in Eq. (5) are *F*= 664 MPa and *n*=0.407. It is confirmed that the cyclic stress-strain relationship could be accurately estimated from the curves produced by this procedure.

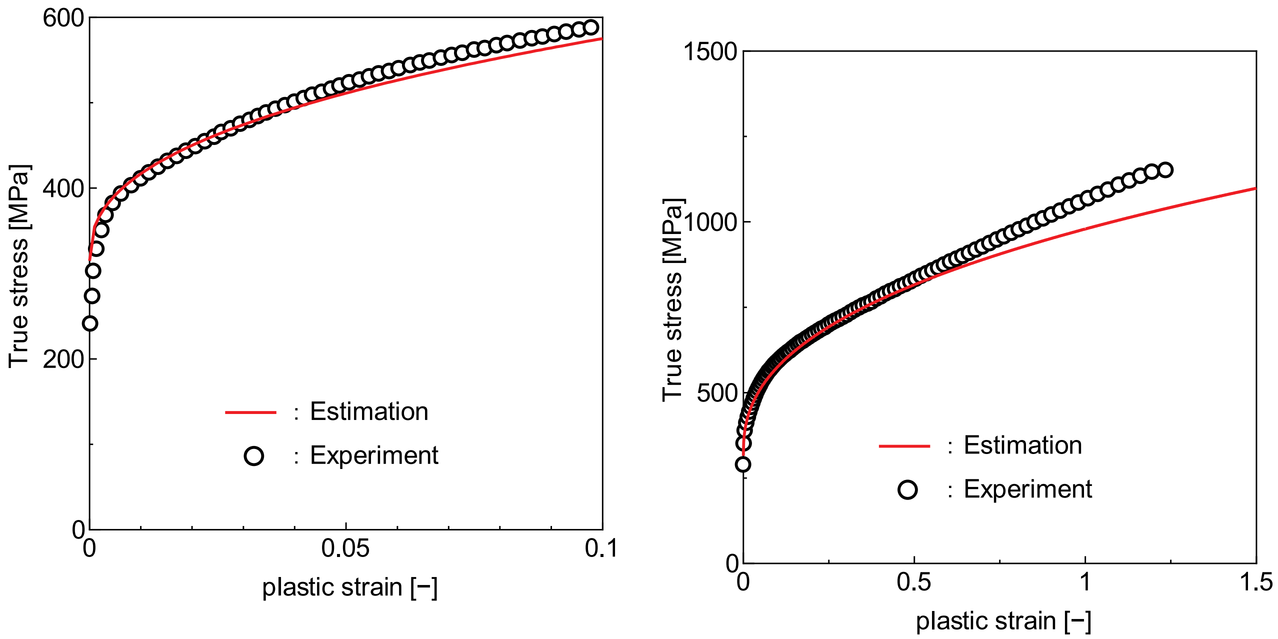

(a) $0 \leq \varepsilon_{pl} \leq 0.1$ (b) $0 \leq \varepsilon_{pl} \leq 1.5$

Fig.1 Estimation of cyclic stress-strain curves.

3. NUMERICAL SIMULATION OF FATIGUE CRACK PROPAGATION

3.1. Theory of crack -combined force models

An overview of numerical simulation of fatigue crack propagation developed by Yamashita et al. [2] is presented briefly. The fatigue crack propagation simulation used in this study is based on the strip yield model that can consider the work-hardening effect of the material. The strip yield model treats the plastic zone formed at the crack tip as a virtual crack and allows the crack opening/closing behaviour near the crack tip to be considered by arranging one-dimensional bar elements. The formulation at maximum load is described. For the formulation of the case where the tip of the plastic zone formed by the current load is still within the plastic zone formed by the previous load at maximum load, and the case at minimum load, see Refs. [1] and [2].

If, at maximum load, the tip of the plastic zone at the current crack length grows forward of the previous maximum plastic zone tip, the superposition of the strip yield model is valid, as shown in Fig. 2.

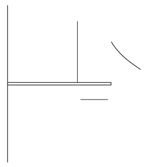

[Notes.]
(a) Problem under consideration,
(b) Stress distribution on the assumed crack line in the crack-free state,
(c) Stress distribution acting on the crack face shown in (b),
(d) Cohesive forces acting on the virtual crack face,
(e) Residual stress distribution on the assumed crack line in the crack-free state,
(f) Residual stress distribution acting on the crack face shown in (e),

a_0 Initial (physical) crack tip,
a current physical crack tip,
c current fictitious crack tip.

Fig.2 Principles of superposition concerning the stress distribution at maximum loading condition.

To account for work-hardening effects, the cohesive force acting in the virtual crack plane is not constant at the yield stress, but the cohesive force distribution acting as ${\sigma_c}^{max}(x)$. From the superposition principle for the cracking problem shown in Fig. 2, the crack opening displacement at position $x = x_j$ on the crack line at maximum load is given by Eq. (6).

$$V_{max}(x_j) = P_{max} \sum_{i=1}^{n} \sigma_s(x_i) F(x_j, x_i, c) - \sum_{i=k+1}^{n} {\sigma_c}^{max}(x_i) F(x_j, x_i, c) + \sum_{i=1}^{n} \sigma_R(x_i) F(x_j, x_i, c) \qquad (6)$$

In the strip yield model, the bar elements embedded in the virtual crack face retain a certain finite length because of residual plastic deformation when the acting stress is unloaded. Gauge length $L_{max}(x_j)$ (the length of the bar element when the acting stress on the bar element is unloaded) at this step is given by Eq. (7) below.

$$L_{max}(x_j) = V_{max}(x_j) / \{1 + \sigma_c^{max}(x_j)/E'\} \qquad (7)$$

One of the authors also showed that the plastic strain of the crack line perpendicular component on the crack line can be expressed as in Eq. (8). The coefficient α_1 in Eq. (8) is considered to depend on the yield stress σ_Y and the work hardening factor H and can be expressed as a function of yield stress and work hardening rate in Eq. (9) [8].

$$\varepsilon_p^{max}(x_j) = \alpha_1 \sqrt{L_{max}(x_j)/x} \qquad (8)$$

$$\alpha_1 = 0.50(H/\sigma_Y {\varepsilon_Y}^{0.5})^{-0.38} \qquad (9)$$

Considering the above results, the crack aperture can be determined by performing the following convergence calculations while updating the distribution of the cohesive forces acting on the crack line.

3.2. Crack propagation analysis

Fatigue crack growth history under some loading conditions is estimated using the fatigue crack growth simulations [2] implementing the material stress-strain relationship presented in the previous chapter.

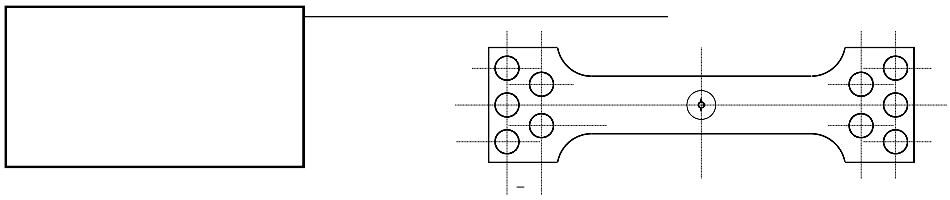

Fig.3 Specimen configuration [1].

Table 4 Loading condition of constant amplitude loading.

Test No.	Stress ratio [-]	Maximum load [kN]	Minimum load [kN]
1	0.05	23.06	1.49
2	0.3	30.42	9.48
3	0.5	36.40	18.53

Table 5 Loading condition of block loading

Test No.	Maximum load reduction ratio ξ [%]	Maximum loads ${P_{max}}^{(1)}$, (${P_{max}}^{(2)}$) [kN]	Minimum load P_{min} [kN]
4	15	20.16, (17.16)	0.33
5	30	20.22, (14.13)	0.39

Table 6 Loading condition of spike loading

Test No.	Spike ratio α [-]	Spike load P_{spike} [kN]	Max. load P_{max} [kN]	Min. load P_{min} [kN]
6	1.5	47.08	31.40	3.14
7	2.0	62.76	31.40	3.14

The loading conditions were carried out for three different loading conditions: constant amplitude loading, block loading and spike loading, the detailed loading conditions are shown in Tables 4 to 6. Center cracked tensile (CCT) specimen with a plate thickness of 4 mm was used. The specimen geometry is shown in Fig. 3. Applied steel is Grade KA36 by ClassNK with a yield stress of 352 MPa for No. 1 to 5 while Grade KA32 steel by ClassNK with a yield stress of 339 MPa was used for No. 6 and 7.

The maximum load reduction ratio is $\xi(= ({P_{max}}^{(1)} - {P_{max}}^{(2)})/{P_{max}}^{(1)} \times 100)$ and the spike ratio is $\alpha(= P_{spike}/P_{max})$.

Comparisons of numerically simulated fatigue crack propagation histories with measured results are shown in Fig. 4. For comparison, numerical simulation results for an elastic-perfectly plastic material is also shown. For constant load amplitude, the fatigue crack growth history is accurately estimated for a stress ratio R of 0.05, given a stress-to-strain relationship corresponding to cyclic loading. On the other hand, for stress ratios R of 0.3 and 0.5, the fatigue crack growth history is estimated faster than the measured values when a stress-strain relationship corresponding to cyclic loading is given. The reason for this is currently unclear, but is assumed to be due to an earlier estimate of the opening of the fatigue crack tip as a result of higher cohesive forces than in the case of the elastic-perfectly plastic assumption shown in blue curves. It is also possible that the calculation of the cohesive forces has not converged sufficiently, and further investigation is required.

On the other hand, the estimation accuracy of fatigue crack propagation history was improved by providing the stress-strain relationship corresponding to cyclic loading under the two-stage block loading and spike loading conditions.

These results confirm that the estimation accuracy of fatigue crack growth history can be improved by providing a stress-strain relationship corresponding to cyclic loading conditions, as proposed in this study.

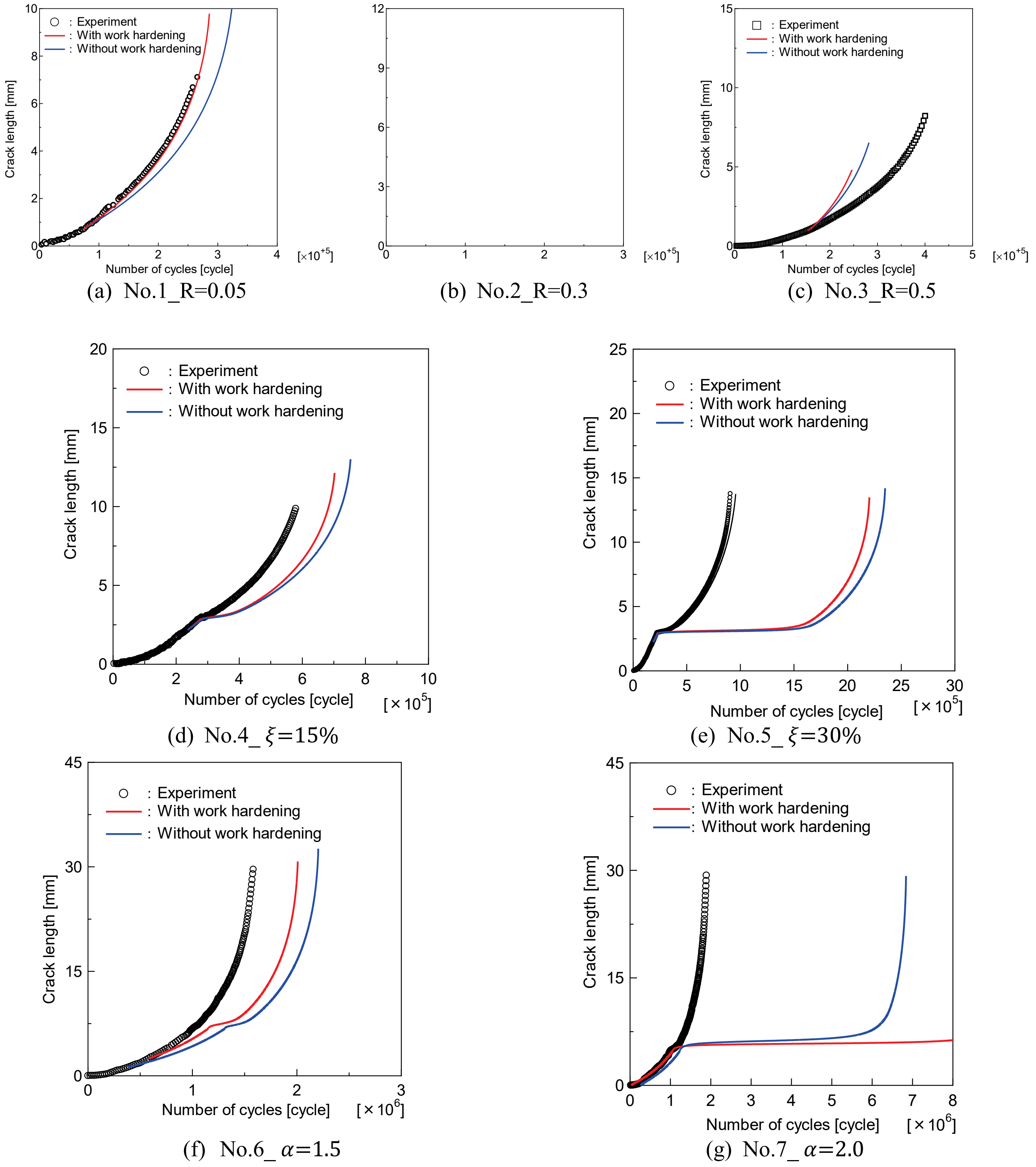

Fig.4 Comparison of fatigue crack growth curves by numerical simulations with measurements.

4. CONCLUSION

To improve the accuracy of crack propagation analysis, fatigue crack propagation analysis was carried out given the cyclic stress-strain relationship given by the method proposed by the authors and compared with the measured results.

As a result, it was confirmed that the estimation accuracy of fatigue crack propagation history was improved by giving the stress-strain relationship under cyclic loading conditions, although some improvements remained in some calculations.

ACKNOWLEDGEMENTS

This work was supported by JSPS Grant-in-Aid for Challenging Research (Exploratory), Grant Number JP 20K21048.

REFERENCES

[1] Toyosada M., Gotoh K., Niwa T., Fatigue crack propagation for a through thickness crack tip, International Journal of Fatigue, **26**, (2003), 983-992.

[2] Yamashita K., Gotoh K., Numerical Simulation of Fatigue Crack Propagation and Crack Opening and Closing Model by Considering the Strain-hardening Effect of Materials, Proceedings of ISOPE 2014, (2014), 151-157.

[3] Shimooka T., Murakami K., Matsuda K., Gotoh K., Experimental investigation of the stress-strain relationship in steels subjected to cyclic loading, Quarterly Journal of the Japan Welding Society, **19**, (2022), 1-4. (in Japanese)

[4] Takaki, S., Yielding and Deformation Behavior in Polycrystalline Ferritic Steel, Journal of Japan Institute of Metals and Materials, **83**, (2019), 107-118. (in Japanese)

[5] D.Akama, T.Tsuchiyama and S.Takaki, Evaluation of Dislocation Density in Cold-Worked Iron as Measured Via X-Ray Diffractometry, Journal of the Society of Materials Science, Japan, **66**,(2017), 522-527. (in Japanese)

[6] Takaki S., Work Hardening in Ferritic Steel, Tetsu-to-Hagane, **105** (2019), 941-956. (in Japanese)

[7] JIS G0551, Steels-Micrographic determination of the apparent grain size, (2020).

[8] Harada K., Gotoh, K., Improvement of the Strip Yield Model Considering the Work Hardening Effect of Materials, The Japan Society of Naval Architects and Ocean Engineers, **14**, (2011), 39-46. (in Japanese)